Lessons Learned from Large-Scale Aerospace Structural Testing

Andrew E. Lovejoy[1], Dawn C. Jegley[2], Mark W. Hilburger[3] and Adam Przekop[4]

Please address all correspondence to Andrew E. Lovejoy, Mail Stop 190,
NASA Langley Research Center, Hampton VA 23681-2199
Andrew.E.Lovejoy@nasa.gov

Abstract

proposed paper to be presented at the 62nd AIAA/ASME/ASCE/AHS/ASC Structures, Structural Dynamics, and Materials Conference with AIAA SciTech 2020
January 5-9, 2021
Nashville, TN

Subject Category: Structures
Historical Lessons Learned and Advances in Structural Applications

I. Introduction

Large-scale testing of representative aerospace structures is used to validate the performance of the structures or to provide full-scale response characteristics for validation of analysis methods. Whenever possible, a building-block approach is commonly used for large-scale testing, where a full-scale test is the culmination of years of research to demonstrate the performance of the final design. In other cases, the full-scale test is used when the proper full-scale response cannot easily be represented by subscale testing, which is particularly true for composite structures where scaled testing is typically not easily accomplished. This paper presents some lessons learned by researchers at the NASA Langley Research Center (LaRC) from large-scale structural testing conducted at LaRC, NASA Marshall Space Flight Center (MSFC), and NASA Armstrong Flight Research Center (AFRC). Test articles examined to provide lessons learned are: the Advanced Composites Technology (ACT) program full-scale 40-ft long stitched composite semi-span wing [1]; the Advanced Air Transport Technology (AATT) project 39-ft long, 27% scale tow-steered passive aeroelastic tailored (PAT) wing [2]; the Shell Buckling Knockdown Factor (SBKF) project full-scale 27.5-ft diameter metallic barrels [3]; the SBKF large-scale 8-ft diameter, 44.5% scale metallic barrels [4]; and the stitched composite Environmentally Responsible Aircraft (ERA) project, 80% scale multi-bay box (MBB) representative of the center section of a hybrid-wing body (HWB) aircraft [5]. This paper provides descriptions of the test articles and the testing conducted, describes problems identified during the testing, defines mitigation approaches to solve the problems where developed, and summarizes the lessons learned.

---

[1] Research Aerospace Engineer, Structural Mechanics and Concepts Branch, Associate Fellow AIAA.
[2] Senior Research Aerospace Engineer, Structural Mechanics and Concepts Branch, Associate Fellow AIAA.
[3] Principal Technologist for Structures, Materials, and Nanotechnology, Space Technology Mission Directorate, Associate Fellow AIAA.
[4] Senior Research Aerospace Engineer, Structural Mechanics and Concepts Branch, Associate Fellow AIAA.

II. Stitched and PAT Wings

The full-scale 40-ft long stitched wing was a carbon fiber/epoxy, resin infused test article with through-the-thickness Kevlar stitches to replace fasteners and suppress damage growth. The stitched wing consisted of the upper and lower covers, leading and trailing edge spars, and ribs. Figure 1 shows the test setup for the stitched wing. The test article was attached to the strongback at LaRC using a set of metallic root mount plates around the perimeter of the test article that were attached to the upper and lower covers and to the leading and trailing edge spars. The upper and lower covers were unitized with the skin, and the stringers and intercostals were stitched together. In addition, stitching was applied in a uniform manner throughout the upper and lower cover skins and the stringers. The leading and trailing edge spars and the ribs were mechanically fastened to the upper and lower covers, and the ribs were also mechanically fastened to the spars. Loads were introduced to the test article using actuators attached to the floor and attached to the test article by pairs of load lines at four spanwise locations with one actuator at the leading edge (shown in Figure 1) and one actuator at the trailing edge. The pair of actuators at the tip were attached to a metallic finishing rib/fixture, and the pair of actuators inboard of the tip were attached to a saddle that encapsulated the test article. These eight load lines were used to apply -1g down-bending and 2.5g up-bending load cases. For the third load case, braked roll, an additional line load was added. This load was applied through a load arm, shown in Figure 1, that was attached to plates on the upper and lower covers to extend downward behind the wing to simulate a landing gear attachment.

The 27% scale tow-steered PAT wing was a carbon fiber/epoxy wing based on a variant of the NASA Common Research Model [6] and included upper and lower skins, leading and trailing edge spars, and 58 ribs. Both skins of the PAT wing were fabricated using tow-steered composites while the spars and ribs were fabricated using conventional composites. Due to numerous manufacturing flaws, including delaminations and wrinkling, a significant repair was made on the leading edge spar where the outboard 11 feet of the composite spar was replaced with an aluminum spar section of nearly equivalent sizing and performance. Figure 2 shows the PAT wing test set-up at AFRC. The wing was mounted to two root reaction plates that were connected to the leading and trailing edge spars using four 3-inch-diameter attachment pins, two in each spar. The root reaction plates were connected to a 6-degree-of-freedom reaction table using angle brackets, with the reaction table supported by load cells at six locations atop a base pedestal. The pedestal was joined to three steel support I-beams that were connected to the load lines, completing a self-reacting test system. Loading was applied using seven pairs of load lines at seven span-wise locations, with one actuator at the leading edge (LE) spar and one at the trailing edge (TE) spar at each spanwise location. The load lines were attached to the test article and support I-beams, except at the wing tip that was attached to the test article and floor, for the -1g down-bending load condition and flexural axis loading at individual load lines. For the 2.5g up-bending load condition, the outboard three sets of load locations were connected to the overhead load structure identified in Figure 2, with the steel overhead load structure connected to the support I-beams. The pairs of wing loads at each outboard station were applied using a single loading actuator for each of the load stations, with the three loading actuators embedded in the overhead load structure. Cables connected the loading actuators to the corresponding pairs of wing load connection points at each of the three spanwise loading locations. The cables were guided by movable pulleys that enabled control of the loading direction at each location. The cables were attached to I-beams that split the load to the two wing connection points in a whiffle tree configuration, with the positioning of each overhead cable connection to the I-beam providing the correct load division between the corresponding two wing connection points.

Both of these tests had similar challenges that led to important lessons learned. First, loading on these two test articles was intended to represent specific loads experienced by the wings during service, aerodynamic and braked roll for the stitched wing, and aerodynamic for the PAT wing. For both of these tests, preliminary analyses were carried out using linear static analysis. However, the deflections of these test articles were large enough that geometric nonlinearity needed to be included in the analysis. Therefore, nonlinear static analysis was conducted for both test articles, and the loads were applied at the actuator connection points as follower loads because that was more representative of the aerodynamic loads on the real wing. However, as seen in Figures 1 and 2, there were conventional load lines that were connected to the test article at one end and a fixed point on the other. Therefore, the applied test loads were actually aligned with the load lines and were not follower forces on test article as would be expected for the aerodynamic loads on the real wing.

Failure to initially model the test load conditions accurately resulted in issues with the original test configuration design. For the stitched wing, the initial analyses model applied loads as follower loads consistent with aerodynamic loads. This modeling method meant that the loads at the tip remained in the plane of the metallic rib/fixture, resulting in in-plane forces only, as desired to best represent flight loads. However, test loads were aligned with the load line, that is, follower forces with respect to the load line orientation and not the test article as would be the case for the aerodynamic loads. When the analysis load was updated to keep the load aligned with the load line, by including beam representations of the load lines and defining the loads as follower loads with respect to those beams, which better represented the test condition, the loads resulted in a combination of in-plane and normal forces on the metallic rib/fixture. The initial design of this metallic rib/fixture was a thick plate. The normal force predicted upon applying the loads consistent with the test configuration resulted in predicted bending stresses sufficient for the metallic rib/fixture to yield. Therefore, as seen in Figure 1, stiffeners were added to the metallic rib/fixture to alleviate the predicted yielding issue. Another issue that arose in both of the tests was response due to eccentric loading. For the stitched wing, the load arm for the braked roll condition was eccentric from the I-beam extending off the back of the test article. That eccentricity was not included in initial test design analyses. When the eccentricity was included in the analysis model the load arm was predicted to bend during the test. Thus, a mitigation was incorporated in the design which connected a load line between the strongback and the load arm to restrain the motion of the load arm to remain in-plane. A similar issue occurred with the PAT wing, where the load lugs to which the load lines were attached were initially modeled as planar, where the actual load line was connected to one side of the load lug for the test. Again, when the eccentricity was included in the final pretest analysis model, excessive bending stresses were predicted that created significant negative margins, while the initial test design analyses did not consider the eccentricity in the analyses where load was applied to the center of the pin hole on the lug in the plane of the load lug (zero eccentricity). The mitigation was to manufacture couplers so that the load line was attached below the load lug to eliminate the eccentricity and to keep the applied load in the plane of the load lug. These examples demonstrate the first lesson learned:

Lesson 1) Analyze the test configuration. While tests are typically designed to apply loads consistent with how loads are applied to the real structure, that is not always the case. Therefore, while analysis of the actual in-service loading scenario is necessary for designing flight structures, analysis of the actual test setup that accounts for load orientation and eccentricity are necessary to adequately design the test, including the test fixture hardware.

The next lesson learned again concerns the applied loading on a test article. In the case of the stitched wing, the load lines began in a vertical position. On the other hand, the PAT wing testing took a different approach. For the up-bending test, where large deflections would occur, the load line orientations were selected so that at the maximum load, the loads would be normal to the surface as predicted by analysis. The orientation at maximum load was obtained using follower forces applied to the model, and then the load lines were configured so that at the expected maximum deflection, the load line axis and the follower loads from the analysis were aligned. For the load lines of the PAT wing at stations 3 and 4 (recall, ordered in pairs from inboard to outboard), the load line bases were attached to the bottom I-beams at a position to produce load lines aligned with follower loads. For the outer sets of load application locations, pairs 5, 6 and 7, AFRC test engineers developed a unique overhead loading structure as indicated in Figure 2. The pairs of loads were applied with spreader bars at each of the three stations in a manner consistent with a whiffle tree configuration. The application included the introduction of three loading actuators to pull the cables combined with three pully position control actuators (see test description above). However, the overhead load structure was designed very early in the project due to scheduling constraints. When the overhead load structure was designed, the predicted displacements were smaller than those eventually observed during the test, and those smaller predicted displacements were used to size the actuator strokes. Also, the motion of the pulley during loading generated additional slack in the line because it shortened the distance that the load cable had to traverse from the actuator, over the pulley, and down to the spreader bars. This shortening of the cable distance created the need for additional stroke of the load application actuator. Lastly, during the testing, the significantly larger displacement exhibited by the test article than expected due to boundary responses required more pulley motion and, therefore, more required load actuator stroke. The overhead loading fixture was designed and constructed prior to when these issues were identified. Thererfore, the additional needed stroke from deformation, combined with the geometry of the overhead load structure, lead to an insufficient stroke in the load actuator to maintain a normal load orientation at maximum load. Rather, the load vector rotated from an inboard orientation (acute angle between load vector and upper cover surface inboard of load application point) to an outboard orientation (obtuse angle between load vector and upper cover surface inboard of load application point). Therefore, the second lesson learned is:

Lesson 2) Design the load application structure with sufficient margin to account for deviations from expected response. Whether for conventional load lines on the stitched wing and inboard on the PAT wing, or the moving overhead load application system used outboard on the PAT wing, predicted load and deflection response should not be close to the limits of the test load structure capabilities. Rather, significant margin should be applied to the predicted limits to ensure that the test setup does not preclude attaining the required test loads. In the case of the overhead structure, the stroke for the load actuators should have had significant margin to account for possible underestimation of wing deflection and cable slack created by movement of the pulleys. Especially since the design for the overhead load structure was done so early in the project and with limited information, a margin of 50% in stroke capability would not have been unreasonable, and would have permitted sufficient stroke to attain the desired load orientation. Additional margins should apply to both stroke and load capabilities, and the amount of margin should be higher for designs finalized earlier in the process when test article responses are more preliminary in nature, and can be smaller for designs developed closer to the test when test article responses are better understood.

The PAT wing is part of other lessons learned associated with boundary measurements introduced and described in Section III with the SBKF full-scale metallic barrels, and self-reacting structures introduced and described in Section IV with the SBKF 8-ft metallic barrels.

III. SBKF Full-scale Metallic Barrels

Two full-scale metallic barrel test articles, designated ETTA1 and ETTA2, were each fabricated from eight existing Space Shuttle external tank (ET) panels to support testing at MSFC to update the buckling-critical launch vehicle structure buckling knockdown factors. The provided ETTA1 and ETTA2 panels were manufactured from Al-Li-2195 flat plate material stock, into which the orthogrid stiffener pattern was machined to form the pockets and weld land details. The flat orthogrid panels were then bump-formed to an Outer Mold Line (OML) radius of 168.0 inches and then heat-treated to their final temper (i.e., the panels were under-formed relative to the final cylinder OML radius of 165.5 inches). The test articles were friction-stir welded using a vertical weld tool at MSFC. Figure 3 shows the test setup for the SBKF full-scale testing. The test configuration comprises the load test annex (LTA) crosshead at the top of the setup, hydraulic load lines, an upper load introduction cylinder (ring and simulator), the test article and attachment rings, the lower load introduction cylinder (ring and simulator), and the LTA floor at the bottom of the test setup. The components between the LTA floor and crosshead, termed the stack, included the LH2 load ring through the load lines, and was nearly 70 feet tall. The LTA crosshead and floor constitute rigid boundaries (i.e., ground) locations. The upper and lower load introduction cylinders were heritage hardware that were developed for testing the ET intertank, and were designed to represent the stiffness of the LO2 tank (upper, or top) and LH2 tank (lower, or bottom). Test loading consisted of various combinations of axial compression, bending, and internal pressure. Load limits for the test system were 2.25 million pounds of axial compression and 1.4 psi internal pressure, and were limited by the capacity of the hydraulic load actuators used for this setup.

The SBKF full-scale barrel tests utilized heritage load introduction structure (upper and lower simulators and rings). While some drawings and information were available for these structures, they were not sufficient to guarantee that they were modeled with sufficient accuracy for test and analysis correlation. The only instrumentation on the simulators for the ETTA1 test were 40 strain gages. Test and analysis correlation for those strain gages was poor, and the analysis predicted bending in the simulators in opposite direction from what was observed in the test. For ETTA2 testing, speckle patterns for the digital image correlation (DIC) system were added to the exterior of the simulators for a short distance, about 12 inches, from the simulator and test article ring interface to help characterize the membrane and bending response. This additional instrumentation still did not provide sufficient data to understand the simulator response and the influence on the test article response. The DIC resolution was insufficient for the small simulator responses because the DIC system was sized for the much larger barrel deformations. Additionally, the DIC data on the exterior could not address the possibility of a gap opening up on the interior of the joint. For the PAT wing, significant DIC data was collected, and that data enabled identification of several load introduction structure responses that led to test and analysis discrepancies. By considering the DIC results and the identified boundary response, some test and analysis correlation errors reduced from about 19% to 4%.

Lesson 3) Characterization of load introduction structure response is critical to understanding test response. Understanding of the load introduction structure response is important in understanding test response because assumptions about the boundary conditions, including load introduction structure, in an analysis can influence predicted responses and lead to poor test and analysis correlation. Instrumenting load introduction structure can provide data that enable identification of unexpected load introduction conditions that can result in poor test and analysis correlation. This consideration may be particularly important when using heritage hardware where a full understanding of the hardware is not available. Therefore, it is advisable to conduct tests on heritage load introduction structure to characterize its performance whenever possible.

Recall that each of the full-scale barrels was formed by friction-stir welding eight panels that had been formed to 168-in. radius and then heat treated. Prior to welding, the panels were presumed to be in a stress-free state, that is, free from residual stresses due to manufacturing. However, the welding process resulted in local residual stresses at the welds and widespread residual stresses in the full barrel due to pulling the panels together to form the 165.5-inch radius of the test article. The residual stresses due to bending from reducing the radius of the panels was particularly significant in the circumferential stiffeners, and those compressive stresses increased from the skin to a maximum at the top edge of the stiffeners. Including residual stresses had a small benefit on global response test and analysis correlation, but had a significant impact improving test and analysis correlation of the local deflections and strains.

> **Lesson 4) Residual stresses can have significant effect on test article response.** Understanding the manufacturing process for the test article and considering residual stresses in test articles is important. Residual stresses in the test article should be included in analyses to improve test and analysis correlation.

IV. SBKF 8-ft Metallic Barrels

As part of the SBKF project, eight large-scale 8-ft diameter metallic barrels were designed and tested. These sub-scale barrels were designed to have representative non-dimensional parameters equal to representative launch vehicle structures [7]. Orthogrid and isogrid stiffener patterns were used, and each barrel consisted of three Al-Li-2195 panels that were machined flat, then bump formed into the 4-ft radius. The barrels were friction stir welded to form the completed test articles.

Testing was conducted at MSFC, and Figure 4 shows the test assembly that was designed, analytically verified, and fabricated to meet program test objectives. The test assembly was a self-reacting load system (termed the stack) comprised of an upper and lower load spider, 16 load struts, upper and lower transition sections, the test article assembly, and 8 load lines. Each load line consisted of a hydraulic cylinder, 4-inch-diameter loading rod (pipe), a load cell, and attachment hardware. The load lines could be controlled independently in load control or stroke (position) control to apply uniform compression or combined compression and bending with a maximum load capability of 1.5 million pounds of axial compression force and 80,000 pounds of axial tension. The test articles were attached to upper and lower load rings using a low-temperature melting point grout and bolts prior to being installed in the stack. During the testing process for the load conditions of axial load, moment load, and combined axial and moment load, the weight of the upper part of the assembly (transition cylinder and spider) was removed from the test article in a tare procedure so that testing began with zero loads applied to the test article.

The SBKF 8-ft metallic barrel tests and the PAT wing test used self-reacting structures. Both of these structures exhibited both rigid body motions and elastic deformation. The upper spider and transition cylinder exhibited rigid body translations and rotations during the barrel tests. The test article and reaction table in the PAT wing test also exhibited rigid body motions during testing. The load lines of the barrel tests exhibited elastic deformations during testing, as did the reaction table, pedestal and the structure connecting the reaction table to the pedestal during the PAT wing testing. Rigid body motions and elastic deformations of the self-reacting structures can introduce loading and global deflection measurement errors. Global deflection measurement errors were significant in the PAT wing testing.

> **Lesson 5) Understand potential rigid body motion and elastic deformation of the self-reacting system.** Failure to account for rigid body motion and elastic deformations in a self-reacting system can lead to poor test and analysis correlation due to differences in the test load introduction and global deflection measurements. Therefore, monitoring of potential rigid body motions by using appropriate instrumentation is necessary to ensure that such test response is known and accounted for in test and analysis correlation. In the case of the 8-ft barrel tests the rigid body motions were deemed to be negligible, but for the PAT wing rigid body motions had a significant influence on the response.

V. Multi-Bay Box (MBB)

The MBB test article was an 80%- scale component representing a section of the most heavily loaded center section portion of the HWB configuration. The MBB comprised 11 pultruded rod stitched efficient unitized structure (PRSEUS) panels that formed the exterior shell and floor members, along with four interior sandwich rib panels that were used to divide the box width into thirds. In an HWB aircraft, the bulkheads would be near the cockpit and near the tail while in the test article, they are only 7 feet apart. The test article was designed so that they would support the same type of loading as would be found in the actual aircraft. Load introduction boxes were added to the test article to mate with the platens in the Combined Loads Test System (COLTS) facility at LaRC and ensure that the load was imparted to the test article in such a way as to avoid failure at these outer rib locations [5]. The test article was mounted between the platens in COLTS, and four load lines connecting the platens applied mechanical loads to the MBB. Air for interior pressure load was introduced into the bottom section of the MBB and holes in the floor separating the top and bottom sections permitted the air to equalize pressure in the MBB. Load conditions consisted of mechanical load only, pressure load only, and combined mechanical and pressure load.

Since the test article contained thin skins and was subjected to compressive loading, buckling was an important consideration. During testing of the MBB, portions of the test article exhibited different response under the same loading condition for different cycles of that loading condition. For example, the upper cover exhibited local buckling of the skins between stiffeners for the up-bending condition that subjected the upper cover to compressive forces. Incorporating as-manufactured imperfections in the analysis has been shown to improve test and analysis correlation, as was seen for the SBKF project. However, as demonstrated by the MBB, even if the imperfections were known and easily incorporated in the predictive analysis, multiple post-buckle equilibria existed for localized responses due to slight variations in testing conditions. If only a few strain gages are used to monitor the response, an ability to develop a comprehensive understanding of the response might be compromised. For example, if a local skin buckling occurs in the direction opposite to the pre-test prediction, the strain test versus analytical prediction comparison would likely show a qualitatively inaccurate response correlation (tension instead compression or vice versa). This can cause confusion when monitoring response during the test and/or in the post-test data analyses. Therefore, acquiring and monitoring full-field measurements should be incorporated in testing in order to understand response complexities associated with non-unique solutions. Such a capability can be accomplished using digital image correlation.

> **Lesson 6) Full-field response measurements are crucial to understanding response where multiple stable equilibria can exist.** Because very small perturbations can result in changes in local buckling patterns, full-field measurements may be necessary to understand the actual local deformation for each loading cycle, particularly for thin-skin or thin-walled structures. The same is true for global buckling of a structure when there are multiple buckling modes with identical or closely spaced eigenvalues. The use of full-field measurements provides robustness in the test data to account for uncertainties in the response.

VI. Summary of Lessons Learned

Large-scale testing is an important part of researching and developing aerospace structures. Representative aerospace structures tests are used to validate the performance of the structures or to provide full-scale response characteristics without having to test a full-scale structure. However, due to the difficulties that can exist in conducting tests, such as representing correct boundary conditions and applying loads, there are certain lessons learned that need to be considered. Presented herein are six lessons learned from several large-scale tests conducted by researchers at LaRC. Lessons learned were:

- **Analyze the test configuration**
- **Design the load application structure with sufficient margin to account for deviations from expected response during testing**
- **Characterization of load introduction structure response is critical to understanding test response**
- **Residual stresses can have significant effect on test article response**
- **Understand potential rigid body motion and elastic deformation of the self-reacting system**
- **Full-field response measurements are crucial to understanding non-unique response**

Researchers and test engineers, from beginner to experienced, should remember these lessons learned when planning and conducting tests and performing test and analysis correlation. The final paper will include details in support of the presented lessons learned, along with appropriate references.

References

[1] Jegley, D. C., Bush, H G., and Lovejoy, A. E., "Structural Response and Failure of a Full-Scale Stitched Graphite-Epoxy Wing," Journal of Aircraft, Vol. 40, No. 6, November-December 2003, pp. 1192-1199.

[2] Jutte, C. V., Wiesemann, C. D., Lovejoy, A. E., and Stafford, B. K., “Static Loads Testing of a High Aspect Ratio Tow-Steered Wingbox,” 2020 AIAA/ASCE/AHS/ASC Structures, Structural Dynamics, and Materials Conference, AIAA Paper 2020-0243, Orlando, FL, January 6 – 10, 2020.

[3] Lovejoy, A. E., Hilburger, M. W and Gardner, N. W., "Test and Analysis of Full-Scale 27.5-Foot-Diameter Stiffened Metallic Launch Vehicle Cylinders," 2018 AIAA/ASCE/AHS/ASC Structures, Structural Dynamics, and Materials Conference, AIAA Paper 2018-1989, Kissimmee, FL, January 8 – 12, 2018.
[4] Hilburger, M. W., Haynie, W. T., Lovejoy, A. E., Roberts, M. G., Norris, J.y P., Waters, W. A., and Herring, H M., "Subscale and Full-Scale Testing of Buckling-Critical Launch Vehicle Shell Structures," AIAA-2012-1688, 53rd AIAA/ASME/ASCE/AHS/ASC Structures, Structural Dynamics and Materials Conference, Honolulu, Hawaii, Apr. 23-26, 2012.
[5] Jegley, D. C., Rouse, M. , Przekop, A., and Lovejoy, A. E., "The Behavior of a Stitched Composite Large-Scale Multi-Bay Pressure Box," NASA/TM-2016-218972, April 2016.
[6] Brooks, T.R., Kenway, G.K.W., Martins, J.R.R.A., "Benchmark Aerostructural Models for the Study of Transonic Aircraft Wings," AIAA Journal, Vol. 56, No. 7, pp. 2840-2855, 2018.
[7] Hilburger, M. W., Lovejoy, A. E., Thornburgh, R. P., and Rankin, C., "Design and Analysis of Subscale and Full-Scale Buckling-Critical Cylinders for Launch Vehicle Technology Development," AIAA-2012-1865, 53rd AIAA/ASME/ASCE/AHS/ASC Structures, Structural Dynamics and Materials Conference, Honolulu, Hawaii, Apr. 23-26, 2012.

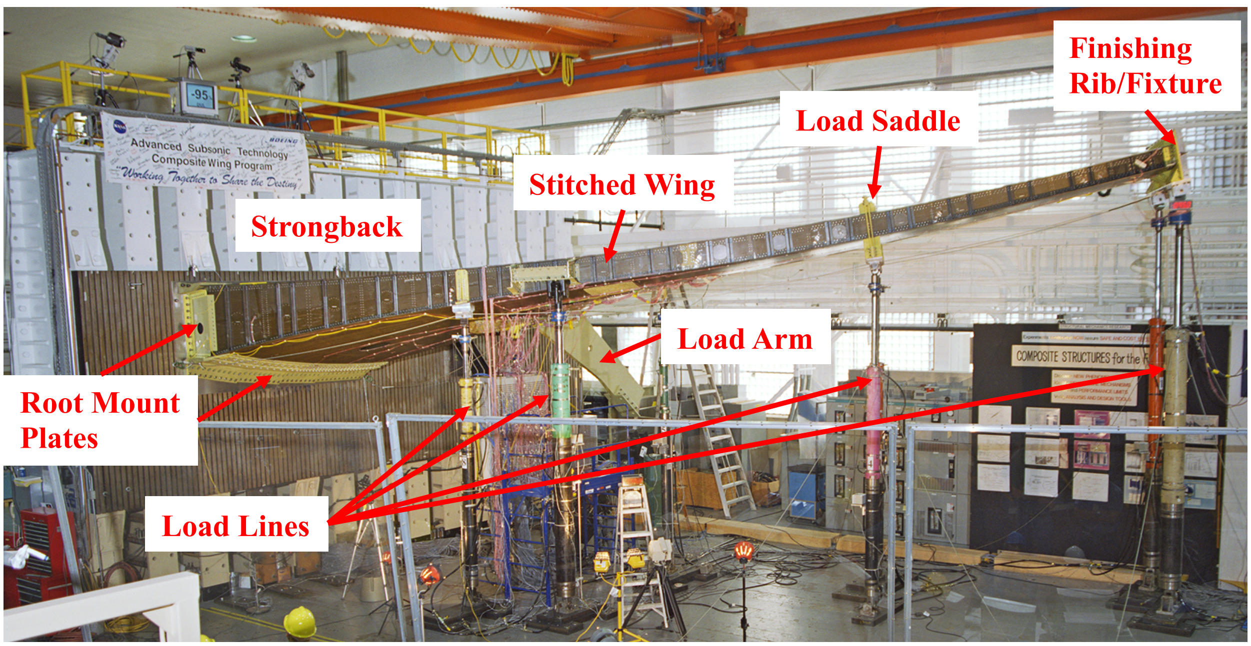

Figure 1. Stitched wing test setup.

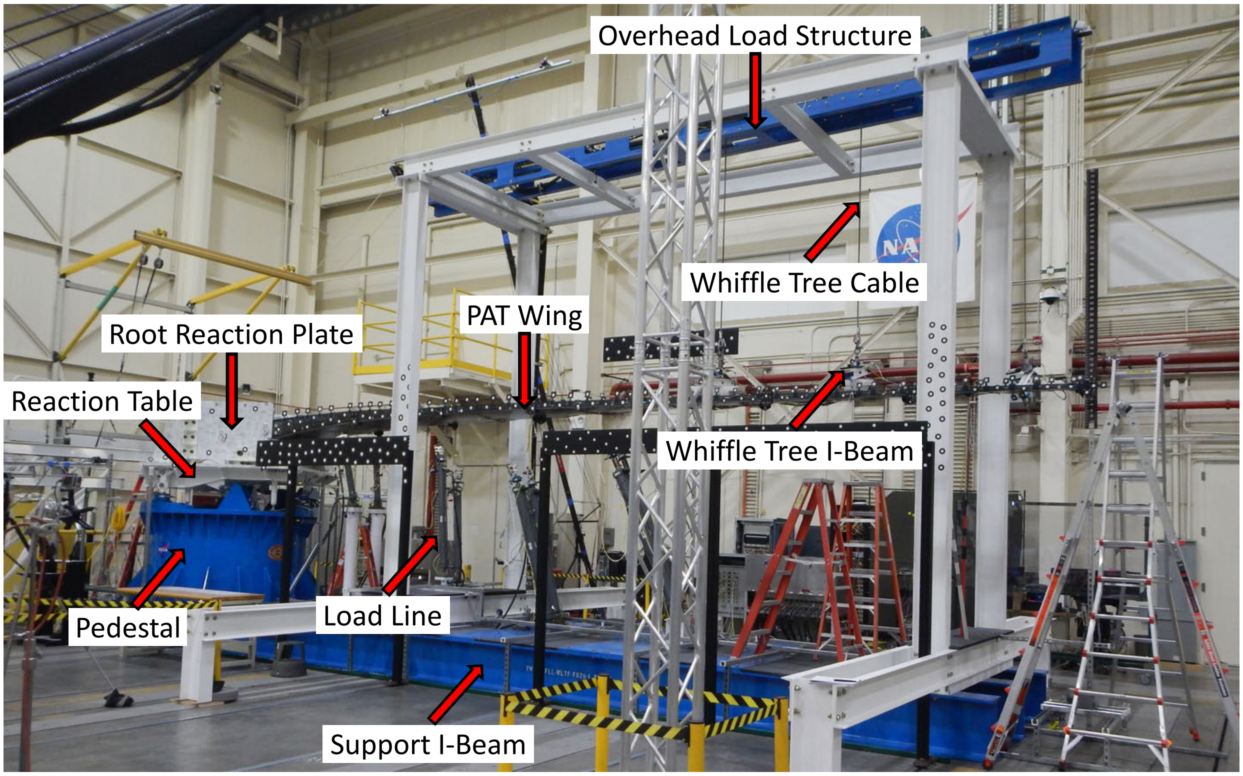

Figure 2. PAT wing test setup.

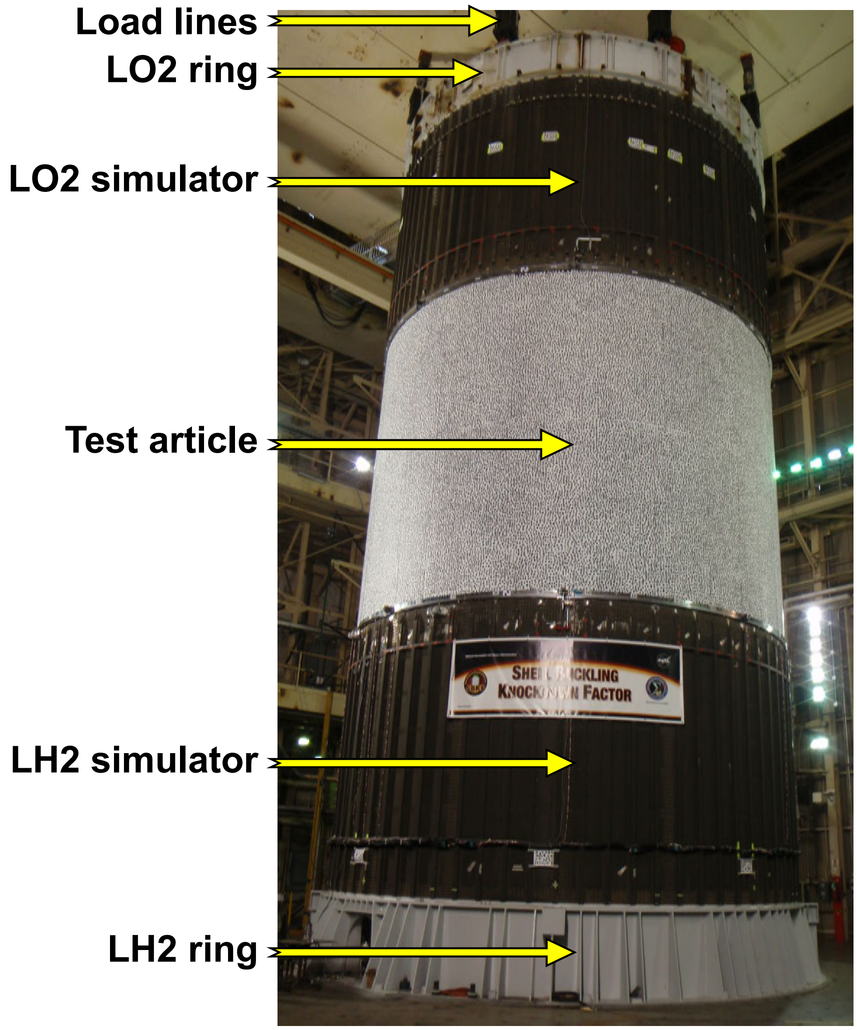

Figure 3. SBKF full-scale metallic barrel test setup.

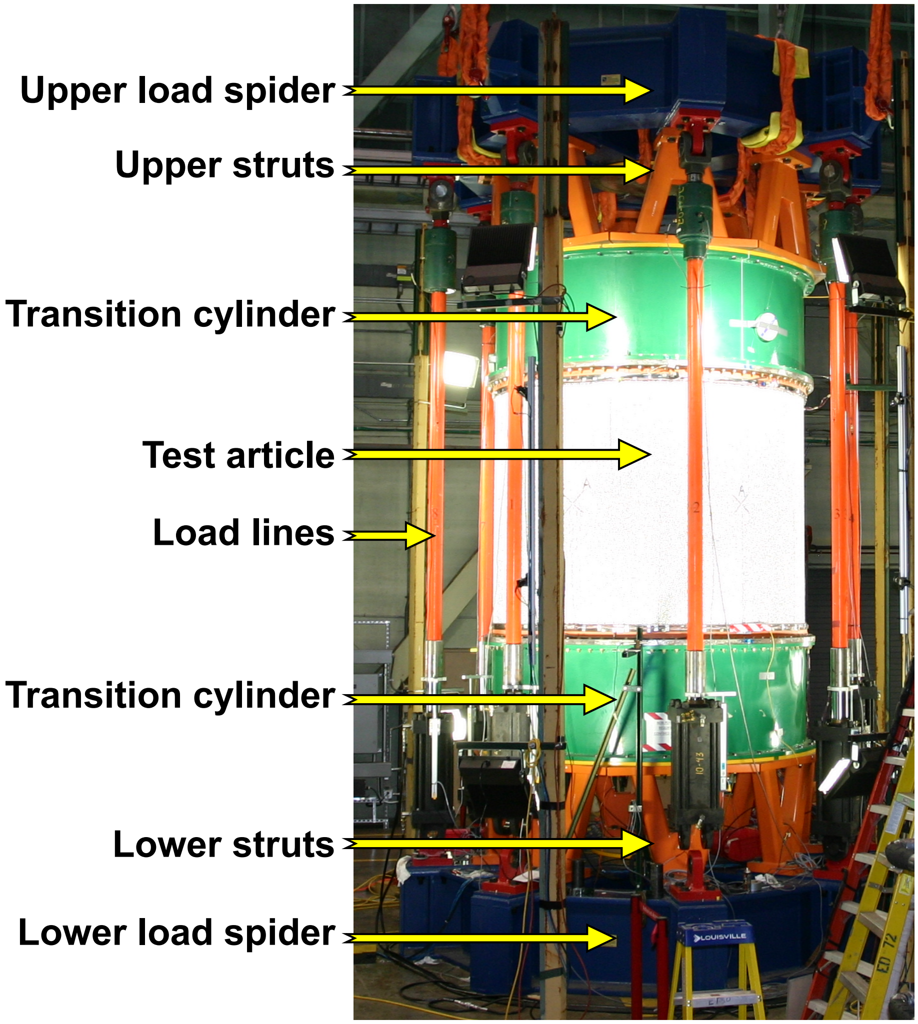

Figure 4. SBKF 8-ft metallic barrel test setup

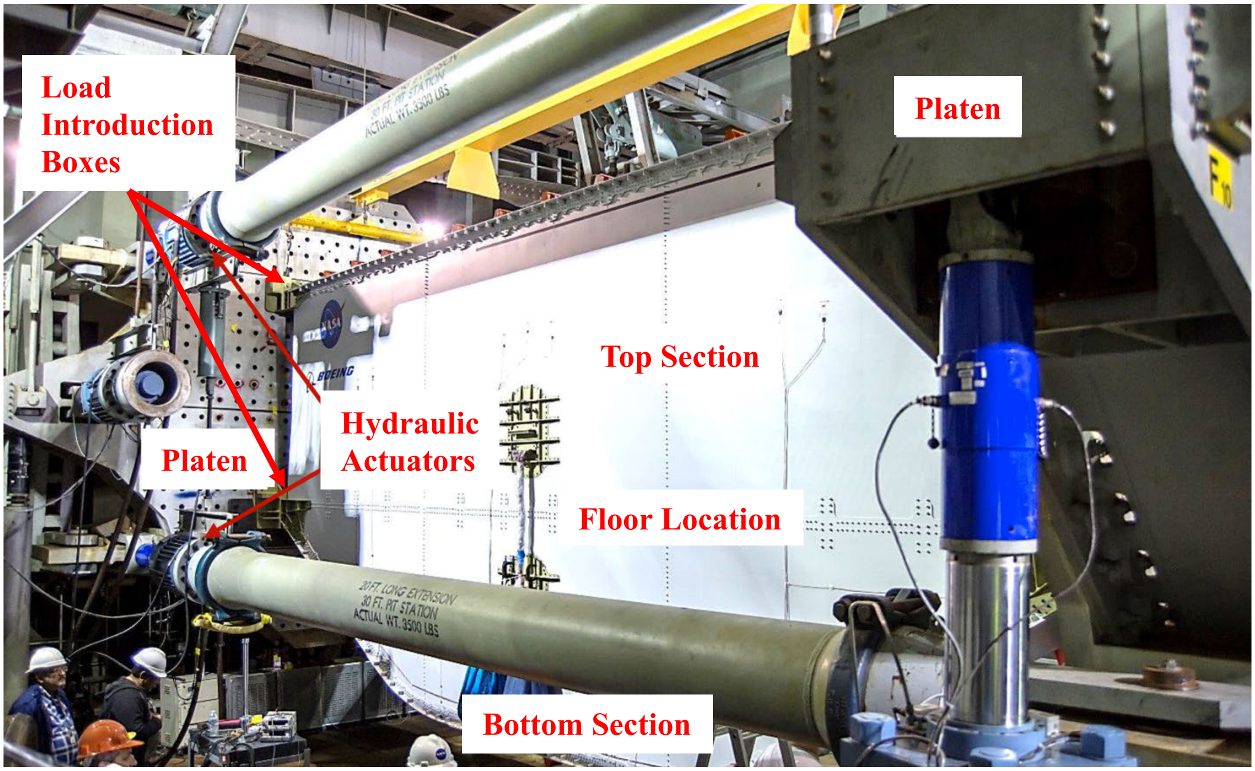

Figure 5. MBB test setup.